# Supporting Information

## Saker et al. 10.1073/pnas.1717646115

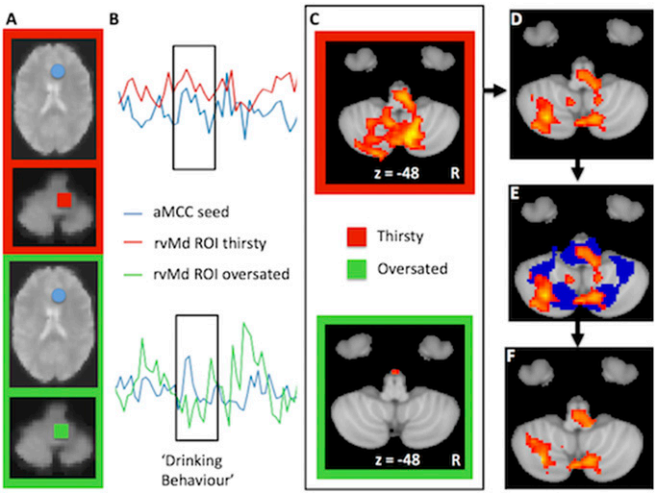


**Fig. S1.** Schematic explanation of PPI contrast between thirsty and oversated conditions. (*A*) BOLD signals were extracted from each voxel in the brain during sequential images acquired in the thirsty (red) and oversated (green) conditions. The aMCC seed used for the PPI analyses is represented by the light blue circles, while the squares represent an example ROI located in the rostral ventral medulla (rvMd) during the thirsty (red) and oversated (green) conditions. (*B*) Voxel-wise analyses were performed to identify regions where signal changes correlated with those of the aMCC seed. For illustrative purposes, data from a single participant is shown. During the thirsty condition, the signal from the example rvMd ROI (red line) is correlated with the signal from the aMCC seed (light blue line) during the period of drinking behavior and not at other times during the experiment. During the oversated condition, in contrast, the signal from the example rvMd ROI (green line) is not correlated with the signal from the aMCC during the period of drinking behavior. (*C*) The outcomes of individual participants' voxel-wise analyses were tested for group effects for the thirsty (red) and oversated (green) conditions. These two images represent the principle functional connectivity analyses for the thirsty and oversated conditions, referred to in the main text. As expected on the basis of the comparison of time courses shown in *B*, the principle functional connectivity analysis for the thirsty condition (red) shows an increase in functional connectivity (correlated activity) between the rvMd ROI and the aMCC during drinking behavior, while no increase is apparent for the principle functional connectivity analysis for the oversated condition (green). (*D*) The principle functional connectivity analyses for each condition were then contrasted to reveal brain regions that showed a greater increase in functional connectivity with the aMCC seed during the period of drinking behavior for one condition relative to the other. This contrast revealed a greater increase in functional connectivity between the rvMd ROI and the aMCC during drinking behavior in the thirsty condition compared with the oversated condition, consistent with the comparison of time courses shown in *B*. (*E*) The contrast between conditions was subsequently masked with the principle activation analysis generated for the thirsty condition (dark blue), which represented regions activated during the period of drinking behavior in the thirsty condition. (*F*) Masking the contrast in this way revealed regions showing both an increase in activation during drinking behavior in the thirsty condition and that showed a greater increase in functional connectivity during drinking behavior in the thirsty condition compared with the oversated condition.

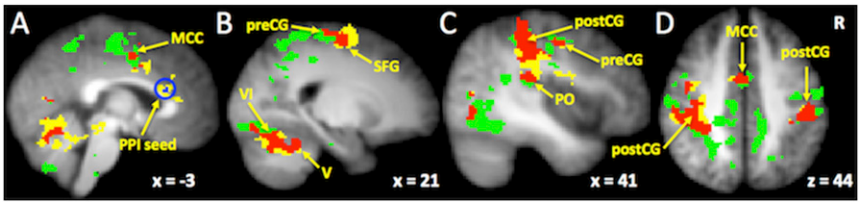


**Fig. S2.** (*A–D*) Logical map comparing regions identified in the PPI analysis for the thirsty condition with regions showing increased activity for the thirsty condition relative to the oversated condition. Green: brain areas showing increased functional connectivity with the aMCC seed in the thirsty condition (thresholded at $z = 3.09$). Yellow: brain activity that was greater for the thirsty condition compared with the oversated condition during drinking behavior. Red: regions that show both properties during drinking behavior. Blue: location of the aMCC seed for the PPI analysis.V, cerebellar lobule V (49); VI, cerebellar lobule VI (49).

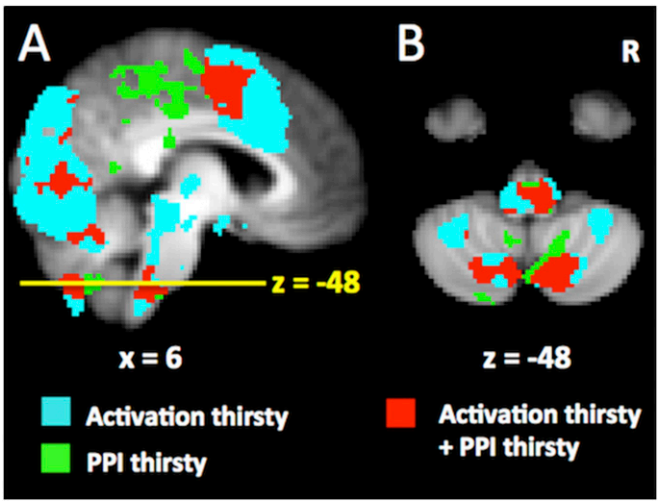


**Fig. S3.** Logical map comparing brain activity during drinking behavior for the thirsty condition and regions identified in the PPI analysis for the thirsty condition. Brain images *A* and *B* correspond to brain images shown in Fig. 2 *B* and *D*. Sagittal image in *A* shows position of the axial slice in *B*. Blue: brain regions activated during drinking behavior for the thirsty condition (thresholded at $z = 3.09$). Green: brain regions showing increased functional connectivity with the aMCC seed during drinking behavior in the thirsty condition (thresholded at $z = 3.09$). Red: regions showing both properties. Note red regions in *B* correspond to brain regions showing greater functional connectivity with the aMCC seed during drinking behavior in the thirsty condition compared with the oversated condition (see Fig. 2*D*). The regions reported in Fig. 2*D* are therefore significantly activated in the thirsty condition and show increased functional connectivity with the aMCC seed during drinking behavior in the thirsty condition.

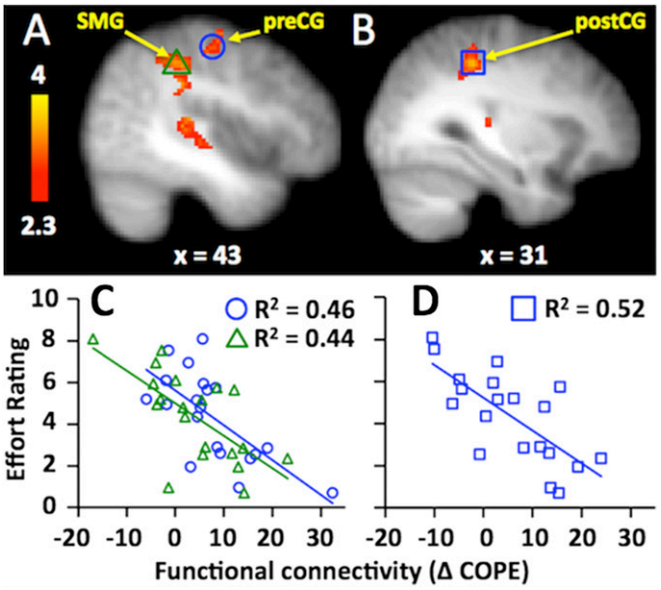


**Fig. S4.** Brain regions showing a negative association between effort ratings and functional connectivity with the aMCC seed during the oversated condition. (*A* and *B*) ROI are represented by blue and green shapes in brain images. All ROIs were selected using the same criteria as the ROI in Fig. 1. (*C* and *D*) Graphs showing the correlation between a participant's effort rating during the oversated condition and functional connectivity with the seed during the same condition. The correlation is derived from the COPEs generated by the PPI analysis. Blue and green shapes correspond to the same shape in brain image shown directly above each graph.

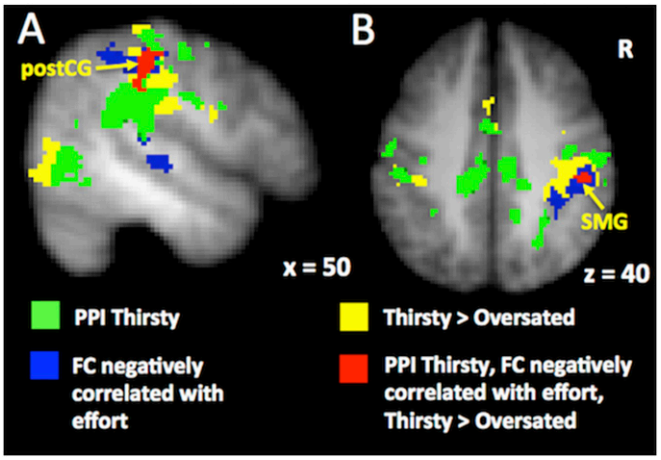


**Fig. S5.** (*A* and *B*) Logical map comparing different imaging analyses performed in the present study. Green: brain regions showing increased functional connectivity with the aMCC seed during drinking behavior in the thirsty condition (thresholded at $z = 3.09$). Yellow: brain regions during drinking behavior with greater activity for the thirsty condition compared with the oversated condition. Blue: brain regions showing increased functional connectivity with the aMCC seed during drinking behavior in the oversated condition that were correlated with effort ratings during this condition; red: regions showing all three properties. Loci in the postCG and SMG contain voxels possessing all three properties.

**Table S1. Brain regions showing significant activation during drinking behavior for the thirsty condition**

| Region | Hemisphere | MNI coordinates | | | *z* Score |
|---|---|---|---|---|---|
| | | *x* | *Y* | *z* | |
| SFG | R | 20 | −2 | 63 | 5.9 |
| SMA | R | 6 | −2 | 64 | 6.0 |
| | R | 4 | 8 | 63 | 5.8 |
| SPL | L | −30 | −52 | 65 | 5.9 |
| | L | −34 | −42 | 57 | 5.9 |
| MCC | R | 6 | 8 | 45 | 6.7 |
| | L | −6 | 8 | 42 | 6.4 |
| PreCG | L | −56 | −8 | 38 | 6.6 |
| | L | −54 | 4 | 20 | 7.0 |
| | R | 58 | −6 | 38 | 6.3 |
| | R | 56 | −2 | 28 | 7.0 |
| PostCG | L | −60 | −18 | 30 | 7.1 |
| | L | −52 | −9 | 26 | 6.8 |
| | L | −64 | −14 | 16 | 7.0 |
| | R | 64 | −10 | 24 | 6.9 |
| aMCC/ACC | L | −2 | 24 | 26 | 6.0 |
| Central operculum | L | −56 | −6 | 12 | 6.7 |
| | L | −42 | −12 | 12 | 6.9 |
| | R | 56 | −10 | 12 | 6.8 |
| PO | L | −42 | −30 | 16 | 6.5 |
| | R | 54 | −32 | 22 | 5.7 |
| Heschl's gyrus | L | −48 | −24 | 12 | 7.1 |
| Anterior insula | R | 36 | 18 | 4 | 7.2 |
| | L | −32 | 22 | 2 | 6.1 |
| Posterior insula | R | 40 | −2 | 4 | 6.5 |
| | L | −42 | −4 | 6 | 6.3 |
| Thalamus | L | −12 | −18 | 4 | 6.5 |
| Cerebellum | R | 24 | −62 | −22 | 7.3 |
| | L | −16 | −66 | −22 | 6.9 |
| | L | −32 | −58 | −28 | 6.3 |
| | R | 18 | −68 | −50 | 6.0 |
| | L | −20 | −66 | −55 | 6.0 |
| RM | L | −6 | −38 | −48 | 6.7 |
| | R | 8 | −36 | −46 | 6.2 |
| Dorsal midbrain | L | −6 | −26 | −6 | 5.7 |

MNI, Montreal Neurological Institute. Anatomical regions selected according to the highest probability provided by the Harvard–Oxford Cortical Structural Atlas, an analytic tool provided by FSL to interrogate fMRI data. Selected voxels: *z* statistic > 5.5 and >50% gray matter, according to the Harvard–Oxford Cortical Structural Atlas. L, left; R, right.

**Table S2. Brain regions showing significant activation during drinking behavior for the oversated condition**

| Region | Hemisphere | MNI coordinates | | | *z* Score |
|---|---|---|---|---|---|
| | | *x* | *y* | *z* | |
| SFG | L | −12 | −2 | 68 | 5.9 |
| SMA/MCC | R | 4 | 8 | 46 | 6.6 |
| | L | −2 | 6 | 46 | 6.0 |
| MCC | R | 6 | 16 | 32 | 6.4 |
| PreCG/PostCG | R | 40 | −14 | 37 | 6.2 |
| | L | −48 | −14 | 35 | 5.7 |
| PreCG | R | 60 | 0 | 27 | 6.4 |
| | L | −56 | −4 | 24 | 6.3 |
| | L | −54 | 6 | 24 | 6.1 |
| PostCG | R | 62 | −16 | 26 | 6.1 |
| | L | −62 | −20 | 28 | 6.2 |
| | L | −64 | −12 | 18 | 7.4 |
| | R | 62 | −8 | 18 | 6.2 |
| Central operculum | R | 60 | −18 | 18 | 6.3 |
| | R | 60 | −10 | 12 | 6.4 |
| | L | −52 | −8 | 4 | 6.8 |
| | L | −40 | −10 | 12 | 7.4 |
| PO | L | −50 | −26 | 12 | 6.5 |
| Posterior insula | L | −38 | −6 | 10 | 6.9 |
| | R | 40 | −2 | 4 | 6.7 |
| Anterior insula | R | 36 | 18 | 4 | 7.0 |
| | L | −32 | 16 | 4 | 5.9 |
| Thalamus | R | 12 | −16 | 0 | 5.8 |
| | L | −12 | −20 | −2 | 5.9 |
| Putamen | L | −20 | 10 | −10 | 6.1 |
| Lingual gyrus | L | −2 | −76 | 6 | 6.1 |
| | R | 8 | −70 | 4 | 6.0 |
| Cerebellum | L | −24 | −70 | −20 | 7.5 |
| | L | −24 | −86 | −20 | 6.7 |
| | L | −38 | −56 | −26 | 5.9 |
| | L | −24 | −68 | −58 | 5.5 |
| | R | 22 | −64 | −20 | 6.1 |
| | R | 14 | −70 | −54 | 5.8 |
| Medulla | R | 6 | −40 | −51 | 5.4 |
| | L | −6 | −38 | −50 | 5.2 |

MNI, Montreal Neurological Institute. Anatomical regions selected according to the highest probability provided by the Harvard–Oxford Cortical Structural Atlas, an analytic tool provided by FSL to interrogate fMRI data. Selected voxels: *z* statistic > 5.0 and >50% gray matter, according to the Harvard–Oxford Cortical Structural Atlas. L, left; R, right.

**Table S3. Brain regions showing greater activation during the drinking behavior for the thirsty condition compared with the oversated condition**

| | | MNI coordinates | | | |
|---|---|---|---|---|---|
| Region | Hemisphere | *x* | *y* | *z* | *z* Score |
| SFG | R | 18 | −4 | 64 | 3.9 |
| SPL | L | −28 | −44 | 64 | 4.3 |
| | R | 30 | −40 | 58 | 3.9 |
| PostCG/SMG | R | 36 | −34 | 42 | 4.1 |
| PostCG | L | −50 | −24 | 48 | 3.4 |
| | L | −38 | −32 | 42 | 4.3 |
| | R | 50 | −26 | 48 | 3.6 |
| SMA/MCC | — | 0 | 0 | 46 | 3.3 |
| MCC | R | 6 | −2 | 44 | 3.2 |
| | R | 1 | 19 | 32 | 3.3 |
| | — | 0 | 4 | 34 | 3.2 |
| aMCC | L | −2 | 26 | 18 | 3.4 |
| ACC | R | 2 | 40 | 8 | 3.5 |
| PreCG | R | 28 | −24 | 68 | 3.9 |
| PO | R | 42 | −26 | 22 | 3.3 |
| Lateral occipital cortex | R | 48 | −70 | −6 | 3.7 |
| Cerebellum | L | −2 | −66 | −12 | 4.6 |
| | L | −28 | −52 | −30 | 3.7 |
| | L | −30 | −52 | −50 | 3.4 |
| | R | 18 | −60 | −18 | 3.7 |
| | R | 26 | −66 | −22 | 3.9 |
| | R | 16 | −48 | −22 | 3.4 |
| Lingual gyrus | L | −8 | −64 | −2 | 3.9 |
| Dorsal midbrain | — | 0 | −26 | −10 | 3.1 |

MNI, Montreal Neurological Institute. Anatomical regions selected according to the highest probability provided by the Harvard–Oxford Cortical Structural Atlas, an analytic tool provided by FSL to interrogate fMRI data. Selected voxels: *z* statistic > 3.0 and >50% gray matter, according to the Harvard–Oxford Cortical Structural Atlas. L, left; R, right.

**Table S4. Brain regions showing increased functional connectivity during drinking behavior in the thirsty condition, relative to nondrinking baseline**

| Region | Hemisphere | MNI coordinates | | | *z* Score |
|---|---|---|---|---|---|
| | | *x* | *y* | *z* | |
| SFG | L | −24 | −4 | 62 | 3.7 |
| PreCG | R | 14 | −22 | 72 | 4.1 |
| | R | 48 | −10 | 50 | 4.0 |
| | R | 60 | 0 | 22 | 4.4 |
| | R | 18 | −26 | 64 | 3.9 |
| | L | −2 | −16 | 60 | 4.4 |
| | L | −38 | −16 | 48 | 4.0 |
| | L | −52 | −6 | 26 | 3.9 |
| PostCG | R | 30 | −36 | 63 | 4.2 |
| | R | 58 | −18 | 38 | 4.4 |
| | R | 40 | −34 | 50 | 4.5 |
| | L | −34 | −29 | 60 | 4.4 |
| | L | −48 | −28 | 44 | 4.0 |
| | L | −54 | −14 | 44 | 4.0 |
| SPL/PostCG | R | 21 | −42 | 65 | 4.4 |
| SPL | L | −24 | −48 | 60 | 4.0 |
| PostCG/SMG | R | 40 | −34 | 50 | 4.5 |
| SMG | R | 62 | −30 | 28 | 4.5 |
| | R | 55 | −41 | 20 | 4.3 |
| SMA | R | 4 | 0 | 54 | 4.3 |
| Posterior cingulate cortex | L | −12 | −32 | 40 | 4.2 |
| | R | 8 | −22 | 40 | 4.0 |
| Precuneous | L | −10 | −57 | 55 | 4.4 |
| | R | 10 | −54 | 54 | 4.0 |
| | R | 12 | −50 | 42 | 3.9 |
| PO | R | 57 | −31 | 24 | 4.3 |
| | R | 56 | −24 | 16 | 4.3 |
| | R | 46 | −30 | 18 | 4.2 |
| | L | −54 | −34 | 24 | 3.8 |
| MCC | — | 0 | −4 | 44 | 4.2 |
| Lateral occipital cortex | R | 46 | −62 | −2 | 4.1 |
| | L | −40 | −70 | −10 | 4.3 |
| Occipital fusiform gyrus | R | 28 | −78 | −10 | 4.2 |
| Cerebellum | L | −38 | −54 | −26 | 4.0 |
| | L | −24 | −80 | −44 | 3.7 |
| | L | −30 | −64 | −56 | 4.1 |
| | R | 28 | −52 | −26 | 3.7 |
| | R | 10 | −64 | −46 | 4.0 |
| RM | R | 2 | −34 | −50 | 3.8 |

MNI, Montreal Neurological Institute. Anatomical regions selected according to the highest probability provided by the Harvard–Oxford Cortical Structural Atlas, an analytic tool provided by FSL to interrogate fMRI data. Selected voxels: *z* statistic > 3.5 and >50% gray matter, according to the Harvard–Oxford Cortical Structural Atlas. L, left; R, right.

**Table S5. Brain regions showing increased functional connectivity during drinking behavior in the oversated condition, relative to nondrinking baseline**

| Region | Hemisphere | MNI coordinates | | | *z* Score |
|---|---|---|---|---|---|
| | | *x* | *y* | *z* | |
| SFG | R | 19 | −4 | 60 | 4.4 |
| PostCG/PreCG | L | −36 | −26 | 52 | 4.4 |
| | R | 39 | −26 | 56 | 4.7 |
| PostCG | L | −30 | −34 | 64 | 4.5 |
| | R | 39 | −28 | 55 | 5.0 |
| | R | 48 | −18 | 44 | 4.7 |
| | R | 40 | −24 | 46 | 4.7 |
| PreCG | R | 2 | −18 | 52 | 4.7 |
| | R | 46 | −10 | 54 | 4.1 |
| | R | 39 | −14 | 40 | 4.4 |
| SPL | L | −18 | −52 | 60 | 4.2 |
| | R | 20 | −48 | 62 | 4.5 |
| | R | 36 | −46 | 60 | 4.4 |
| | R | 32 | −42 | 48 | 4.7 |
| SMG | R | 62 | −28 | 26 | 4.6 |
| SMA | R | 6 | 4 | 58 | 4.2 |
| | L | −4 | −6 | 50 | 4.4 |
| Posterior cingulate cortex | R | 4 | −22 | 46 | 4.7 |
| Precuneous | R | 8 | −52 | 52 | 4.5 |
| | R | 12 | −68 | 32 | 4.5 |
| | L | −2 | −68 | 34 | 4.5 |
| | L | −6 | −48 | 38 | 3.8 |
| PO | L | −54 | −32 | 24 | 4.4 |
| | R | 58 | −22 | 16 | 4.4 |
| | R | 44 | −28 | 18 | 4.3 |
| Planum temporale | R | 58 | −26 | 14 | 4.6 |
| Lateral occipital cortex | L | −56 | −64 | 6 | 4.3 |
| | R | 50 | −70 | 6 | 3.9 |
| Intracalcarine cortex | L | −10 | −76 | 8 | 4.3 |
| Lingual gyrus/occipital fusiform gyrus | R | 16 | −78 | −8 | 4.5 |
| Lingual gyrus | R | 12 | −88 | −4 | 4.9 |
| | R | 21 | −56 | −12 | 4.3 |
| Occipital fusiform gyrus | L | −26 | −70 | −14 | 4.3 |
| Thalamus | L | −8 | −18 | 2 | 3.9 |
| | R | 8 | −18 | 2 | 3.7 |
| Cerebellum | L | −10 | −60 | −16 | 4.3 |
| | L | −20 | −56 | −22 | 4.1 |
| | R | 23 | −52 | −18 | 4.6 |
| Ventrolateral medulla | R | 16 | −16 | −10 | 3.8 |
| Rostral pons | R | 2 | −20 | −22 | 3.7 |
| | L | −6 | −24 | −22 | 3.7 |
| Mid pons | R | 8 | −24 | −32 | 4.1 |
| | L | −10 | −26 | −30 | 3.8 |
| Lateral mid pons | R | 14 | −28 | −36 | 3.8 |

MNI, Montreal Neurological Institute. Anatomical regions selected according to the highest probability provided by the Harvard–Oxford Cortical Structural Atlas, an analytic tool provided by FSL to interrogate fMRI data. Selected voxels: *z* statistic > 3.5 and >50% gray matter, according to the Harvard–Oxford Cortical Structural Atlas. L, left; R, right.

**Table S6. Brain regions showing increased functional connectivity, relative to the nondrinking baseline, during drinking behavior that was also greater in the thirsty condition compared with the oversated condition**

| | | MNI coordinates | | | |
|---|---|---|---|---|---|
| Region | Hemisphere | *x* | *y* | *z* | *z* Score |
| Cerebellum | L | −40 | −52 | −44 | 3.0 |
| | L | −28 | −66 | −50 | 3.8 |
| | L | −16 | −60 | −58 | 3.8 |
| | L | −22 | −54 | −56 | 3.2 |
| | L | −10 | −58 | −54 | 3.4 |
| | — | 0 | −72 | −48 | 3.4 |
| | R | 10 | −70 | −48 | 3.5 |
| Rostral lateral medulla | R | 10 | −40 | −46 | 3.6 |
| Rostral medial medulla | — | 0 | −34 | −48 | 3.2 |
| RM | R | 4 | −36 | −48 | 3.2 |

Anatomical regions selected according to the highest probability provided by the Harvard–Oxford Cortical Structural Atlas, an analytic tool provided by FSL to interrogate fMRI data. Selected voxels: *z* statistic > 3.0 and >50% gray matter, according to the Harvard–Oxford Cortical Structural Atlas.

**Table S7. Brain regions showing a negative association between effort ratings and increased functional connectivity with the aMCC seed during drinking behavior in the oversated condition, relative to the nondrinking baseline**

| | | MNI coordinates | | | |
|---|---|---|---|---|---|
| Region | Hemisphere | *x* | *y* | *z* | *z* Score |
| PreCG | R | 44 | −10 | 60 | 3.0 |
| PostCG | R | 32 | −34 | 46 | 3.5 |
| | R | 46 | −19 | 50 | 3.1 |
| SMG | R | 46 | −30 | 42 | 3.9 |
| Planum temporale | R | 44 | −28 | 12 | 3.3 |
| Heschl's gyrus | R | 36 | −24 | 10 | 3.2 |
| Superior temporal gyrus | R | 52 | −24 | 0 | 3.0 |

Anatomical regions selected according to the highest probability provided by the Harvard–Oxford Cortical Structural Atlas, an analytic tool provided by FSL to interrogate fMRI data. Selected voxels: *z* statistic > 3.0 and >50% gray matter, according to the Harvard–Oxford Cortical Structural Atlas.